

A THEORETICAL MODEL OF A LOSSY DIELECTRIC SLAB FOR THE CHARACTERIZATION OF RADAR SYSTEM PERFORMANCE SPECIFICATIONS

Gregory L. Charvat, MSEE
Prof. Edward J. Rothwell, PhD
Department of Electrical and Computer Engineering
Michigan State University
2120 Engineering Building
East Lansing, MI 48825

ABSTRACT

Some radar applications require a system to acquire range profile or S11 network analyzer data through a lossy dielectric layer to measure something behind that lossy dielectric layer. It is often difficult to specify the dynamic range requirements of such a system due to the “flash” of initial reflected transmitted energy from the lossy dielectric layer. It is also difficult to determine the most effective architecture for such a system, such as pulse IF, ultra-wideband impulse, FMCW, or another more exotic architecture. In this paper a theoretical model is developed of a lossy dielectric layer, a radar transmitter and receiver, and a standard radar target on the other side of the lossy dielectric layer. The theoretical results from this model provide insight into the dynamic range requirements for any radar system that must acquire range profile data or S11 network analyzer data through a lossy dielectric of any permeability, permittivity, and conductivity at any microwave or RF frequency range in order to measure something behind that lossy dielectric layer.

Keywords: Radar Scattering, Radar System Performance, Radar System Specifications, Measurement Through a Lossy Dielectric, Scattering from a Lossy Dielectric

1. Introduction

When developing specifications and deciding on architectural requirements for a test system (radar, S11 network analyzer, etc) that must measure through a lossy dielectric it is often difficult to decide on such issues as dynamic range and radar mode. In this paper, a theoretical planar model of a lossy dielectric, air, and metal sheet is developed (see figure 1). Using this model, theoretical range profiles are created to characterize dynamic range requirements for such a test system when it is required to measure a metal sheet as a radar target on the opposite side of a lossy dielectric and air layer.

The theoretical model presented in this paper was solved based on planar waveguide and circuit theory. Problem solving procedures and concepts for solving such

theoretical models are well known [1, 2, 3, 4, 5]. An example of previous work in this area would be in [6], where a metal cylinder inside of a lossy dielectric box was imaged theoretically, then imaged in the lab using real data. In this case, the lab results closely matched that of the theoretical.

In order to keep this theoretical study practical, it was decided to present the theoretical data in the form of range profiles. Where, a radar (or S11 network analyzer) chirp signal from 250 MHz to 3 GHz was simulated, and the time domain range profile results of the scattered field presented. Such range profile results are easily recognizable to anyone in the field.

The geometry of this theoretical study is described in section 2. Section 3 outlines the problem solving strategy. Section 4 presents the spatial frequency domain Fourier transform pairs used throughout the derivation. Section 5 steps through each step of the theoretical problem being solved. Section 6 presents theoretical results in the form of range profile data. Section 7 summarizes the results and discusses future work. All references are indicated in section 8.

2. Geometry

The geometry of this theoretical study is shown in figure 1. This is an infinitely planar problem, and thus each of the layers are infinite in the x y plane. The line source is infinite in the x direction and located at $y = 0, z = 0$. Region 1 between $b \leq z \leq t$ contains the infinite plane lossy dielectric of finite thickness. Region 2 between $t \leq z \leq 0$ is free space. Region 3 at $z \geq 0$ is free space. Region 4 between $d \leq z \leq b$ is also free space. The last layer covering $z \leq d$ is an infinite planar perfect electric conductor (PEC) for use as the metal sheet radar target.

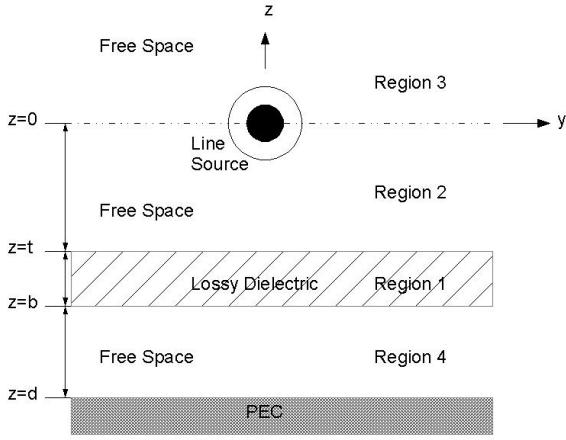


Figure 1: Geometry.

3. Problem Solving Strategy

This planar problem is solved by utilizing the time harmonic Maxwell's equations, and spatial frequency domain analysis. There are several steps required for solving such a problem, these are outlined below:

1. Define the line source.
2. Model the problem as fields in terms of vector potentials and find the wave equations.
3. Convert to the spatial frequency domain and find the ordinary differential equations.
4. Find the solutions to the ordinary differential equations in each region.
5. Apply the boundary conditions.
6. Solve each of the constants, n equations and n unknowns.
7. Solve for the fields in region 3.
8. Take the inverse spatial frequency Fourier transform to get the time harmonic solution.
9. Take the inverse Fourier transform of the time harmonic solution to get the time domain radar range profile solution.

4. Spatial Frequency Domain Fourier Transform Pairs

As indicated in step 3 of section 3, the time harmonic wave equations must be converted to the spatial frequency domain by Fourier analysis. Shown below are the Fourier transform pairs for this process, these will be referred to throughout this paper:

$$\tilde{A}_x(k_y, z) = \int_{-\infty}^{\infty} A_x(y, z) e^{-jk_y y} dy \quad (1)$$

$$A_x(k_y, z) = \frac{1}{2\pi} \int_{-\infty}^{\infty} \tilde{A}_x(k_y, z) e^{jk_y y} dk_y \quad (2)$$

Where: A_x = vector magnetic potential
 \tilde{A}_x = spatial frequency domain vector magnetic potential
 k_y = spatial frequency

5. Solving the Problem

The first step in solving this problem is in defining the line source according to the geometry in figure 1:

$$\vec{J}(y, z) = \hat{x} I \delta(z - h) \delta(y - 0) \quad (3)$$

Calculate the surface current density:

$$\vec{K}(y) = \lim_{\Delta \rightarrow 0} \int_{h-\Delta}^{h+\Delta} \vec{J}(y, z) dz = \hat{x} I \delta(y - 0) dz \quad (4)$$

Where: $h = 0 - t$ source height above the lossy dielectric

The fields in terms of magnetic vector potential functions:

$$E_x = -j\omega A_x(y, z)$$

$$H_y = \frac{1}{\mu_0} \frac{\partial A_x(y, z)}{\partial z} \quad (5)$$

$$H_z = \frac{-1}{\mu_0} \frac{\partial A_x(y, z)}{\partial y}$$

Define the wave equation for free space regions 2, 3, 4:

$$\nabla^2 A_x + k_0^2 A_x = 0 \quad (6)$$

Define the wave equation for lossy dielectric region 1:

$$\nabla^2 A_x + k^2 A_x = 0 \quad (7)$$

Where the wave numbers in equations 6 and 7 are:

$$k_0^2 = \omega^2 \mu_0 \epsilon_0 \quad \text{for regions 2, 3, 4} \quad (8)$$

$$k^2 = \omega^2 \mu_0 \varepsilon \quad \text{for region 1} \quad (8)$$

Where: $\omega = 2\pi f$

$f =$ radar frequency

$\mu_0 = 12.5656E - 7$ (H/m)

permeability of free space

$\varepsilon_0 = 8.854E - 12$ (F/m) permittivity
of free space

$\varepsilon = \varepsilon_0 \varepsilon_r - j \frac{\sigma}{\omega}$ complex permittivity

of dielectric region 1

$\sigma =$ conductivity in S/m of the lossy
dielectric

$\varepsilon_r =$ relative permittivity of the lossy
dielectric

Take the spatial Fourier transform of the wave equations 6 and 7 with respect to y using equation 1. Thus, the wave equations become the ordinary differential equations (ODE's):

$$\left(\frac{\partial^2}{\partial z^2} + p^2 \right) \tilde{A}_x(k_y, z) = 0 \quad \text{for regions 2, 3, 4} \quad (9)$$

$$\left(\frac{\partial^2}{\partial z^2} + q^2 \right) \tilde{A}_x(k_y, z) = 0 \quad \text{for region 1} \quad (10)$$

Where p^2 and q^2 are defined as:

$$p^2 = k_0^2 - k_y^2 \quad (11)$$

$$q^2 = k^2 - k_y^2 \quad (12)$$

Using equation 1, the spatial Fourier transform was taken of the line source surface current density equation 4, resulting in:

$$\tilde{k}_x = I \quad (13)$$

The solutions to the ODE's 9 and 10 are well known plane wave functions in rectangular coordinates, and can be found in texts such as [7]. From the plane wave functions in [7] we have the following solutions of the ODE's for each region:

$$\text{Region 3, } z \geq 0: \quad \tilde{A}_x = c_1 e^{-jpz} \quad (14)$$

$$\text{Region 2, } t \leq z \leq 0: \quad \tilde{A}_x = c_2 e^{+jpz} + c_3 e^{-jpz} \quad (15)$$

$$\text{Region 1, } b \leq z \leq t: \quad \tilde{A}_x = c_4 e^{+jqz} + c_5 e^{-jqz} \quad (16)$$

$$\text{Region 4, } d \leq z \leq b: \quad \tilde{A}_x = c_6 e^{+jpb} + c_7 e^{-jpb} \quad (17)$$

Where p is defined as:

$$p = \pm \sqrt{k_0^2 - k_y^2} \quad (18)$$

Where the following must be obeyed due to physical reality: $\text{Re}\{p\} > 0$ and $\text{Im}\{p\} < 0$

Where q is defined as:

$$q = \pm \sqrt{k^2 - k_y^2} \quad (19)$$

Where the following must be obeyed due to physical reality: $\text{Re}\{q\} > 0$ and $\text{Im}\{q\} < 0$

Using equation 5, and region dependent ODE's 14 through 17 for the spatial frequency vector potentials, apply the boundary conditions at the interface of each layer. Where, the tangential electric and magnetic fields are continuous. This involves numerous simple algebraic steps which will not be presented here. The result of all boundary conditions solved is a set of 7 equations and 7 unknowns, where the c_n 's are the unknowns:

$$c_1 = c_2 + c_3 \quad (20)$$

$$\frac{\mu_0 I}{jP} = c_1 + c_2 - c_3 \quad (21)$$

$$c_2 e^{+jpt} + c_3 e^{-jpt} = c_4 e^{+jqt} + c_5 e^{-jqt} \quad (22)$$

$$p[c_2 e^{+jpt} - c_3 e^{-jpt}] = q[c_4 e^{+jqt} - c_5 e^{-jqt}] \quad (23)$$

$$c_4 e^{+jqb} + c_5 e^{-jqb} = c_6 e^{+jpb} + c_7 e^{-jpb} \quad (24)$$

$$q[c_4 e^{+jqb} - c_5 e^{-jqb}] = p[c_6 e^{+jpb} - c_7 e^{-jpb}] \quad (25)$$

$$c_6 e^{+jpd} + c_7 e^{-jpd} = 0 \quad (26)$$

We must algebraically manipulate equations 20 through 26 to find a solution for only c_1 since we are only interested in solving for the fields in region 3 (see region 3 ODE equation 14). If we were wanted to solve for other regions, we would have to find more of the solutions to the c_n 's. Thus, the solution to c_1 was found to be:

$$c_1 = \frac{\mu_0 I}{2jp} \left[1 + e^{+jp(2t)} \frac{1-Y}{1+Y} \right] \quad (27)$$

Where Y is an arbitrary constant equation, containing many variables and a result of algebraic manipulation of equations 20 through 26:

$$Y = \frac{q \left[e^{+jqd} - e^{-jq(d-2b)} \frac{1-X}{1+X} \right]}{p \left[e^{+jqd} + e^{-jq(d-2b)} \frac{1-X}{1+X} \right]} \quad (28)$$

Where X is an arbitrary constant equation, containing many variables and a result of algebraic manipulation of equations 20 through 26:

$$X = \frac{p \left[e^{+jpb} + e^{-jp(b-2d)} \right]}{q \left[e^{+jpb} - e^{-jp(b-2d)} \right]} \quad (29)$$

Substitute equation 27 into equation 14 to find the spatial frequency vector potential function (ODE) for region 3:

$$\tilde{A}_x = \frac{\mu_0 I}{2jp} \left[1 + e^{+jp(2t)} \frac{1-Y}{1+Y} \right] e^{-jyz} \quad (30)$$

Take the inverse spatial Fourier transform by substituting equation 30 into equation 2:

$$A_x = \frac{1}{2\pi} \int_{-\infty}^{\infty} \frac{\mu_0 I}{2jp} \left[1 + e^{+jp(2t)} \frac{1-Y}{1+Y} \right] e^{-jyz} e^{+jk_y y} dk_y \quad (31)$$

Apply the following Fourier transform identity from [4] to equation 31:

$$\frac{1}{\pi} \int_{-\infty}^{\infty} \frac{e^{-jy|z-h|}}{p} e^{jk_y y} dk_y = H_0^{(2)}(k_0 r) \quad (32)$$

Where: $H_0^{(2)}$ = the Hankel function of the 2nd kind of order 0.

And, for this case: $r = \sqrt{z^2 - 0^2} = |z|$

In applying the identity equation 32 to equation 31, the result is the time harmonic vector magnetic potential function for region 3:

$$A_x(y, z) = \frac{\mu_0 I}{4\pi j} H_0^{(2)}(k_0 |z|) + \frac{\mu_0 I}{4\pi j} \int_{-\infty}^{\infty} \frac{e^{-jp(z-2t)}}{p} \frac{1-Y}{1+Y} e^{+jk_y y} dk_y \quad (33)$$

Thus, equation 33 is the solution to all the time harmonic fields in region 3. In order to find specifically the electric or magnetic fields, simply plug equation 33 into equation 5. A discrete quadrature integration routine such as those found in MATLAB could be utilized to evaluate the integral in equation 33.

The time domain impulse response of the lossy dielectric planar problem is found by taking inverse Fourier transform of the time harmonic electric field in equation 5. Where, radio waves are incident on the lossy dielectric, and scattered off the dielectric, air, and the infinite planar PEC on the other side (see figure 1).

6. Theoretical Data

In order to keep this theoretical study on the practical side of things, it was decided to use the results from section 5 to create theoretical radar range profile data to see what a radar system or S11 network analyzer might expect to measure when presented with a geometry such as that shown in figure 1.

Equation 33 was modified so as to ignore the principal source contribution of the incident field due to the line source. This is done by simply taking out the Hankel function, the result being:

$$A(y, z) = \frac{\mu_0 I}{4\pi j} \int_{-\infty}^{\infty} \frac{e^{-jp(z-2t)}}{p} \frac{1-Y}{1+Y} e^{+jk_y y} dk_y \quad (34)$$

Practical theoretical results for the electric field in region 3 were then calculated. Looking at figure 1, the values for the geometry were chosen to be:

$$\begin{aligned}
 t &= -5 \text{ feet} \\
 b &= -5.3048 \text{ feet} \\
 d &= -10 \text{ feet} \\
 \text{observation point} &= \{y = 0.1 \text{ feet}, z = 0.1 \text{ feet}\}
 \end{aligned}$$

By applying equation 33 to equation 5, the time harmonic electric field in region 3 was found. The current source value $I = 1$ was used. The integral in equation 33 was evaluated using the MATLAB complex quadrature integration function “quadv.” Frequency dependent permittivity and conductivity parameters were utilized from [8]. The frequency sweep for the time harmonic results was from 250 MHz to 3 GHz. The inverse Fourier transform was then taken of the time harmonic electric field resulting in the impulse response of the scattering from the lossy dielectric, air, PEC layered problem. These impulse range profile results are shown in figures 2 and 3.

Figure 2 shows the real valued time domain range profile data of the impulse scattering off the lossy dielectric, air, PEC layered problem. It is clear from figure 2 that the wall appears at 10 nS as expected by the geometry. It is also clear from figure 2 that the PEC appears at a little more than 20 nS, as expected from a wave traveling round trip through a dielectric region, into air, reflecting off a PEC, and back again. The locations of the lossy dielectric and the PEC in round trip time are indicated in figure 2.

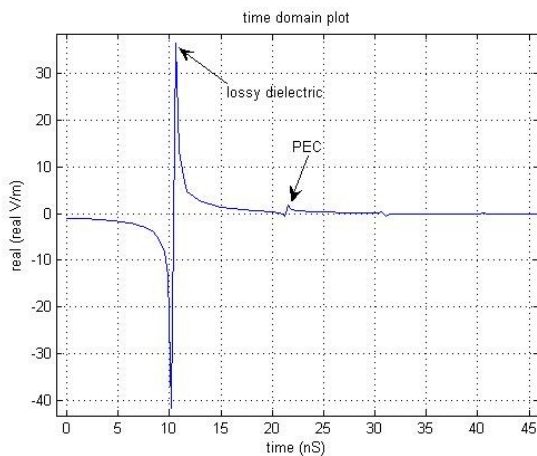


Figure 2: Real valued time domain range profile results.

Figure 3 shows the log magnitude time domain range profile data of the impulse scattering off the lossy dielectric, air, PEC layered problem. This plot is of particular interest for anyone in the field of radar imaging

and involved with determining system specifications. Shown more clearly in this log magnitude plot, the wall appears at 10 nS as expected by the geometry. And also more clearly, the PEC appears at a little more than 20 nS, as expected from a wave traveling round trip through a dielectric region, into air, reflecting off a PEC, and back again. The locations of the lossy dielectric, the back side of the lossy dielectric, and the PEC are indicated in figure 3.

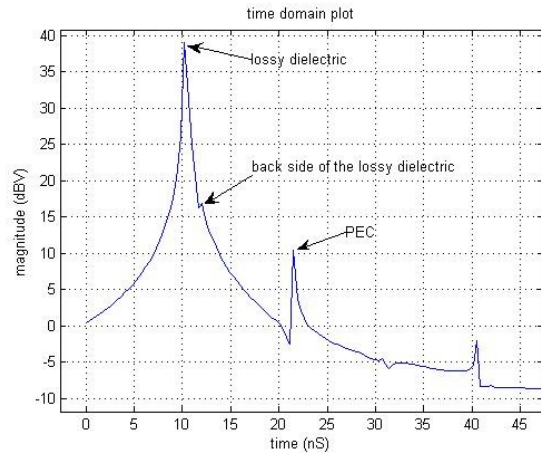


Figure 3: Log magnitude time domain range profile results.

From the results shown here it can be concluded that if a radar system or S11 network analyzer operating in the 250 MHz to 3 GHz range were to detect a very large metal plate on the opposite side of a very large lossy dielectric, separated by air between the metal plate and the lossy dielectric using this geometry, then that radar system would need a minimum dynamic range of 28.7 dB.

7. Conclusions and Future Work

This theoretical study has presented a technique for modeling the dispersive effects of a lossy dielectric. These were shown for the case of an infinite PEC radar target, where in order to measure the scattering from such a PEC sheet on the other side of a lossy dielectric, a radar system operating in the frequency range of 250 MHz to 3 GHz must have a minimum dynamic range of 28.7 dB. Future work will include modifying this theoretical study to include more complex shapes such as corner reflectors and cylinders. Such results have the potential for furthering the understanding of radar scattering of radar targets on the opposite side of a lossy dielectric. Such results will be useful in determining the dynamic range, radar mode, and frequency specifications of future measurement systems that are required to measure something on the opposite side of a lossy dielectric.

8. REFERENCES

- [1] R. Collins, *Field Theory of Guided Waves*. New York: IEEE Press, 1990.
- [2] A. Ishimaru, *Electromagnetic Wave Propagation, Radiation, and Scattering*. New Jersey: Prentice-Hall, 1996.
- [3] J. A. Kong, *Electromagnetic Wave Theory*. Hoboken, NJ: John Wiley and Sons, 1990.
- [4] W. C. Chew, *Waves and Fields in Inhomogeneous Media*. New York: IEEE Press, 1999.
- [5] L. B. Felsen, and N. Marcuvitz, *Radiation and Scattering of Waves*. New York: IEEE Press, 1994.
- [6] M. Schacht, E. J. Rothwell, C. M. Coleman. "Time-Domain Imaging of Objects Within Enclosures." IEEE Transactions on Antennas and Propagation, Vol. 50, No. 6, June 2002, pp 895-897.
- [7] C. A. Balanis, *Advanced Engineering Electromagnetics*. New York: John Wiley and Sons, 1989.
- [8] U. B. Halabe, K. Maser, and E. Kausel, "Propagation Characteristics of Electromagnetic Waves in Concrete, Technical Report." AD-A207387, March 1989.